AIP | Applied Physics Letters

Composite electrolyte with proton conductivity for low-temperature solid oxide fuel cell

Rizwan Raza, Akhlaq Ahmed, Nadeem Akram, Muhammad Saleem, Majid Niaz Akhtar, Tauqir A. Sherazi, M. Ajmal Khan, Ghazanfar Abbas, Imran Shakir, Munazza Mohsin, Farah Alvi, Muhammad Sufyan Javed, M. Yasir Rafique, and Bin Zhu

Citation: Applied Physics Letters **107**, 183903 (2015); doi: 10.1063/1.4934940
View online: http://dx.doi.org/10.1063/1.4934940
View Table of Contents: http://scitation.aip.org/content/aip/journal/apl/107/18?ver=pdfcov
Published by the AIP Publishing

Composite electrolyte with proton conductivity for low-temperature solid oxide fuel cell

Rizwan Raza,[1,2,a)] Akhlaq Ahmed,[1] Nadeem Akram,[1] Muhammad Saleem,[1] Majid Niaz Akhtar,[1] Tauqir A. Sherazi,[3] M. Ajmal Khan,[1] Ghazanfar Abbas,[1] Imran Shakir,[4] Munazza Mohsin,[5] Farah Alvi,[1] Muhammad Sufyan Javed,[1,6] M. Yasir Rafique,[1] and Bin Zhu[2,7,b)]

[1]*Department of Physics, COMSATS Institute of Information Technology, Lahore 54000, Pakistan*
[2]*Department of Energy Technology, Royal Institute of Technology, KTH, Stockholm 10044, Sweden*
[3]*Department of Chemistry, COMSATS Institute of Information Technology, Abbotabad 22060, Pakistan*
[4]*Sustainable Energy Technologies (SET) center, College of Engineering, King Saud University, PO-BOX 800, Riyadh 11421, Kingdom of Saudi Arabia*
[5]*Department of Physics, Lahore College for Women University, Lahore, 54000, Pakistan*
[6]*Department of Applied Physics, Chongqing University, Chongqing 400044, People's Republic of China*
[7]*Hubei Collaborative Innovation Center for Advanced Organic Chemical Materials, Faculty of Physics and Electronic Science/Faculty of Computer and Information, Hubei University, Wuhan, Hubei 430062, China*

(Received 3 June 2015; accepted 11 October 2015; published online 3 November 2015; publisher error corrected 6 November 2015)

In the present work, cost-effective nanocomposite electrolyte (Ba-SDC) oxide is developed for efficient low-temperature solid oxide fuel cells (LTSOFCs). Analysis has shown that dual phase conduction of O^{-2} (oxygen ions) and H^{+} (protons) plays a significant role in the development of advanced LTSOFCs. Comparatively high proton ion conductivity (0.19 s/cm) for LTSOFCs was achieved at low temperature (460 °C). In this article, the ionic conduction behaviour of LTSOFCs is explained by carrying out electrochemical impedance spectroscopy measurements. Further, the phase and structure analysis are investigated by X-ray diffraction and scanning electron microscopy techniques. Finally, we achieved an ionic transport number of the composite electrolyte for LTSOFCs as high as 0.95 and energy and power density of 90% and 550 mW/cm^2, respectively, after sintering the composite electrolyte at 800 °C for 4 h, which is promising. Our current effort toward the development of an efficient, green, low-temperature solid oxide fuel cell with the incorporation of high proton conductivity composite electrolyte may open frontiers in the fields of energy and fuel cell technology. © *2015 AIP Publishing LLC*.
[http://dx.doi.org/10.1063/1.4934940]

At the present time, global energy demand is ever increasing to fulfil the basic needs of the rapidly growing population. Currently, the world is facing energy crises due to the soaring development of industries, rapid urbanization, and unexpected population growth. These energy demands are predicted to increase by roughly 50% in the time frame of 2005 to 2030 as the world population is almost doubling every 35 years, although the rate of increase differs in different countries.[1,2]

Nowadays, researchers and scientists are facing the great challenge of developing sustainable and environmentally friendly energy resources.[3] In order to overcome the global shortage of heat and power, fuel cells and hydrogen are seen as promising possible alternatives.[4] The overall electrochemical conversion efficiency of fuel cells is 80%, which is much higher than that of other power plants, which have an efficiency of around 40%.[5] Among the various types of fuel cells, solid oxide fuel cells (SOFCs) are of particular interest due to their fuel flexibility and higher efficiency, and they are considered as promising power-generation devices.[6,7] In general, a fuel cell consists of three layers, where the electrodes (anode and cathode) are porous and the electrolyte is dense. Among these three layers, the electrolyte is the most important layer of the fuel cell since its ionic conductivity plays a key role in the overall fuel cell performance. The high operating temperature (800–1000 °C) of the yttrium stabilized zirconia (YSZ) electrolyte required to achieve high oxygen ion conductivity in the fuel cell is the main limitation of conventional SOFCs. Hence, for FC products to gain commercial success, the foremost aim is to maintain a lower operating temperature without compromising the efficiency of the device.[8]

The main reason for the higher operating temperature is to increase the number of oxygen ions by the reduction process in the cathode of the SOFC and to transport the oxygen ions through an ion-conducting electrolyte. However, at lower temperatures, the efficiency of the SOFC may be limited because of its poor oxygen-ion conductivity. In order to resolve this challenge, a possible solution is to develop high oxygen-ion conductivities by using nanocomposite electrolytes instead of pure materials, e.g., Gadolinium doped ceria (GDC), Yttrium stabilized zirconium (YSZ), Samarium doped ceria (SDC), etc., in the fuel cell.

Proton conductors are very attractive due to their higher efficiency, low activation energy, and higher fuel utilization factor. Researchers have investigated various approaches to synthesize and enhance both proton and ion conductivity in fuel cells at the same time, for example, Zhao *et al.*[9] Elleuch explored an oxalate co-precipitation process,[10] Richter used

a)razahussaini786@gmail.com
b)binzhu@kth.se and zhubin@hubu.edu.cn

a solid state reaction method,[11] Zhu *et al*. used a wet chemical method,[12] many researchers have used co-precipitation methods,[13–15] and so on.

Although many researchers have developed proton and oxygen ion conductors, few of them have developed mixed ions (oxygen ions and proton ions) in electrolyte materials. Jacquin and colleagues developed proton-conducting $BaCe_{0.9}Y_{0.1}O_{2.95}$ ceramic oxide and achieved a conductivity of BCeYO of up to 1.2×10^{-2} s/cm at 500 °C.[16] Medvedev and colleagues used the solution combustion synthesis method to obtain nanosized powders of $Ce_{0.8}Sm_{0.2}O_{2-\delta-x}$ $BaCe_{0.8}Sm_{0.2}O_{3-\delta}$.[17] Single ion conductor-based electrolytes have not been completely successful, however, in reducing the operating temperature to a lower level.

Another attempt was made by Zhu *et al*.,[12] who introduced the NANCOFC (nanocomposites for advanced fuel cells, www.nanocofc.com) approach, whereby co-ions or hybrid ions were introduced, which not only enhanced the ionic conductivity but was also succeeded in low-temperature SOFCs (LTSOFCs) and was evidently far better than the conventional electrolytes. Therefore, interest in the development of hybrid ion conductors has increased noticeably among the scientific community.[12–14]

In our current work, a two-phase barium-based electrolyte with high ionic conductivity is developed by the wet chemical method and shows a promising trend for LTSOFCs. The barium-based nanocomposites showing high hybrid oxygen and proton (O^{2-}/H^{+}) conductivity at low temperatures have been discovered.

The nanocomposite electrolytes (Ba-SDC, i.e., samaria doped ceria–barium, etc.) are synthesized by the wet chemical method. The stoichiometric molar ratios of the chemicals Ba $(NO_3)_2$, Sm $(NO_3)_3 \times 6H_2O$ (Sigma-Aldrich, USA), and Ce $(NO_3)_3 \times 6H_2O$ (Sigma-Aldrich, USA) were used to synthesize the Ba-SDC nanocomposite electrolyte material. The first solution of $Ce_{0.8}Sm_{0.2}O_{2-\delta}$ is prepared in DI water, and later, a solution of Ba $(NO_3)_2$ is added drop wise to the former one. The most favourable molar ratio of Ce:Sm:Ba = 4:1:1 was selected for preparing a 0.1 mol l^{-1} solution. The as-prepared powder was dried in the oven at a temperature of 110 °C for 1 h, and this homogeneous powder was then sintered at 800 °C for 4 h in air. Finally, the synthesized powder was ground for 20 min using a manual milling apparatus.

A solid state reaction was observed during the preparation of nanocomposite electrodes for the fuel cell. For a single-layer fuel cell, Li_2CO_3 (Sigma-Aldrich, USA), $CuCO_3 \times Cu(OH)_2$ (Sigma-Aldrich, USA), $NiCO_3 \times 2Ni(OH)_2 \times 6H_2O$ (Sigma-Aldrich, USA), and Zn $(NO_3)_2 \times 6H_2O$, in an appropriate molar ratio of 1:2:5:5, were ground together before sintering at 800 °C for 4 h in air. In the last step, the Li Cu Ni Zn O (LCNZ) and electrolyte powder were again ground very thoroughly to avoid any non-homogeneity in the prepared material.

A pellet of pure electrolyte powder with a diameter of 13 mm and thickness of 1 mm was made to measure the conductivity of the prepared composite material. In order to prepare laboratory button cells, after sintering, the obtained powders were uniaxially pressed into pellets in the symmetrical order of anode (LCNZ and Ba-SDC)/electrolyte (Ba-SDC)/cathode (LCNZ and Ba-SDC). The LCZN (electrode) and Ba-SDC (electrolyte) were mixed at a ratio of 50 vol. % for the preparation of both the anode and the cathode. The pellets were pressed under a pressure of 280 kg-cm^{-2} using a mechanical hydraulic press machine. In the last step, the as-prepared pellets were sintered at 650 °C for 1 h to remove any impurities and defects from the final products. Further electrical measurements of the as-prepared fuel cell were carried out by applying the silver paste on both sides of the cell as the current collector.[18]

DC conductivities were measured by a digital micro-ohmmeter (KD 2531, China) in a hydrogen and air atmosphere. The conductivity was calculated with the following formula:

$$\sigma = L/RA,$$

where σ is the conductivity, L is the thickness of the pellet, R is the internal resistance, and A is the area of the cell. The active area of the pellet is assumed to be 0.64 cm^2.

The X-ray diffraction (XRD) pattern of the sintered BSDC (electrolyte) was recorded by an X-ray diffractometer (Rigaku D/Max-2500, Tokyo, Japan) with Cu K_α radiation ($\lambda = 1.5418$ Å) at room temperature with a current of 30 mA and voltage of 35 kV. The phase and structure of the BCDS were determined by means of JCPDs cards. The crystallite size (D_β) was calculated by Scherrer's equation

$$D_\beta = 0.89\lambda/\beta \operatorname{Cos} \theta,$$

where λ and β are the wavelength and full-width at half-maximum (FWHM), respectively.

In order to get an insight into the morphology of nanostructure samples, the scanning electron microscopy (SEM, Philips XL-30) was used.[19,20]

The performance of the fuel cell is executed in the temperature range of 400–600 °C. The electrochemical measurements of the cell are made with hydrogen gas as fuel. The gas flow rate is adjusted with the help of a gas flow meter and set at 100 ml min^{-1} at atmospheric pressure. The fuel cell pellets are fixed in a stainless steel fuel cell device and later sealed with the silicon paste. After the application of load resistance, the values of voltage, current, and open circuit voltage (OCV) are adjusted and measured with the help of a fuel cell testing instrument (SM-102, Tianjin, China). The evaluation of the performance of the cell is further assessed by comparing the IV and IP characteristics curves in the temperature range of 400–600 °C.

In order to study the ionic behaviour and transport mechanism, the electrochemical impedance spectroscopy (EIS) was carried out by implementing VersaSTAT 2273 (Princeton Applied Research, USA) in a hydrogen and air atmosphere. For the EIS data, the frequency ranged from 0.01 Hz to 1 MHz under 10 mV. The obtained data were simulated with software (Z SimpWin, Princeton Applied Research, USA) to draw the appropriate equivalent circuit for the cell.

Thermal expansion was measured with a pushrod dilatometer (402 C, Netzsch, Germany). This dilatometer was equipped with a SiC furnace, which was able to operate

between room temperature and 1600 °C. In this dilatometer, a vacuum-tight system allows measurements to be carried out in pure inert or oxidizing atmospheres, as well as under vacuum. Some primary parameters were set, for example, fused silica, sapphire, tungsten, platinum, and so on, for length calibration. The standard was used to compare the results of the expansion of the specimen and the temperature range of the measurement. Further, the data were analyzed by MS-Windows Thermal Analysis. The software includes semi-automatic routines for correction of the sample holder expansion, as well as onset and peak temperatures, and computation of the expansion coefficients, rate of expansion, inflection points, and so on.

In the thermal expansion analysis of the sample (Ba-SDC) measured in air, three steps were detected at 286, 440, and 590 °C (extrapolated onsets). The sample had continually expanded over the entire temperature range for better accuracy of the results. When the same sample was measured in a Varigon atmosphere, however, two steps were observed at 277 and 432 °C (extrapolated onsets). In this case, the sample had expanded to a maximum at 634 °C with an expansion rate of 0.7%.

The structure of the Ba-SDC nanocomposites is determined from the XRD pattern by means of JCPDs cards. Figure 1(a) describes the XRD profile of the composite Ba-SDC powder. The chemical composition of composite electrolyte sintered at 800 °C is also determined by XRD analysis. The structure of the as-prepared Ba-SDC shows two phases. Samarium-doped ceria-oxide and barium-doped samarium-oxide are found to be cubic in structure and shape due to the presence of peaks [(111) at 28.51] and [(320) at 29.32] for samarium doped ceria-oxide and barium doped samarium-oxide, respectively.

The particle size of each phase was calculated with the help of Scherrer's equation, from which the average particle sizes were estimated to lie in the range of 47–78 nm. The crystal lattice was found to be slightly larger due to the exchange of smaller Sm^{+3} ions (radius = 0.102 nm with coordination number 7) for larger Ba^{2+} ions (radius = 0.138 nm with coordination number 7). This may be attributed to the formation of the grain boundaries present in the Ba-SDC nanocomposite samples.

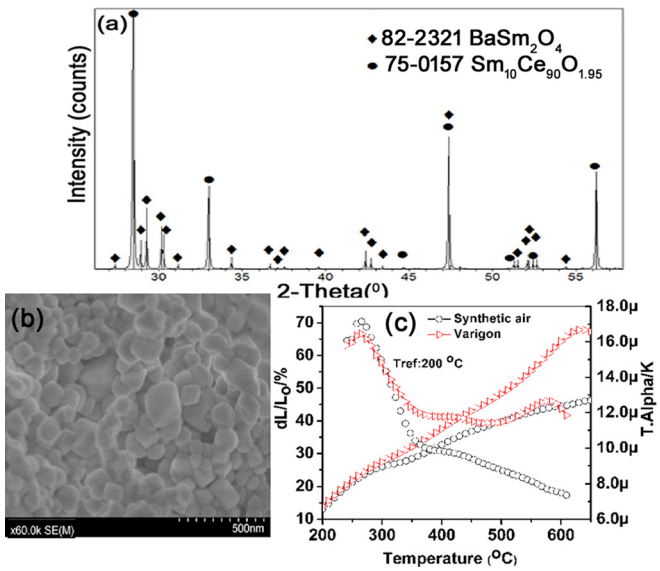

FIG. 1. (a) X-Ray diffraction pattern for BaSDC-carbonate composite electrolyte (b) SEM images of BaSDC-carbonate (c) Thermal expansion of sample (BaSDC-carbonate) measured in air and Varigon.

The microstructure analysis of the surfaces of the nanocomposite electrolyte Ba-SDC oxide powder was performed using SEM, and the respective results are displayed in Figure 1(b). The SEM image in Figure 1(b) shows that the material comprises homogenous agglomerates and the particle size is in the range of 60–100 nm. This range of particle size and fine morphology of nanocomposite electrolyte Ba-SDC oxide can be obtained by fine tuning the sintering temperature, a skilled preparation technique, and an appropriate time as well.

The dense surface of the Ba-SDC oxide nanocomposite electrolyte had smaller grains at multiple junctions, and this conglomeration formed the larger grains on the surface. High temperature calcinations led to excessive agglomeration and grain growth due to their large volume fraction of high-energy inter-crystalline regions without a diffusion barrier. Consequently, no pores are present on the surface of the samples, which is beneficial for the rapid transportation of protons, oxygen, and carbonate ions within the cell. The interfacial region between the Ba-oxide and samarium-doped ceria plays a key role in the overall material conductivity and the cell performance. Recently, it has been found that the conductivity and fuel cell performance are enhanced due to the improvement of the surface morphology, interfacial resistance, and smaller particle size. All of the above mentioned factors facilitate the transportation of protons, oxygen, and carbonate ions transportation.

Figure 1(c) shows the thermal expansion and values for the coefficient of thermal expansion (Tref. = 200 °C) of a co-doped ceria sample. The measurements are done in both air and Varigon atmospheres. Thermal expansion of the sample (Ba-SDC) was measured in air, and three steps were detected at 286, 440, and 590 °C (extrapolated onsets). The sample had expanded over the entire temperature range. Thermal expansion of the sample (Ba-SDC) measured in Varigon atmosphere showed two steps at 277 and 432 °C (extrapolated onsets). It can be seen that sample expands up to a maximum at 634 °C with an expansion rate of 0.7%, which leads to a very slight decrease in sample length until the end of the measurement. The density of the electrolyte was measured using Helium-pycnometry (AccuPyc 1340, Micromeritics, USA). The density of the prepared sample was estimated to be 90% higher due to the existence of the porous structure of material and the appropriate sintering conditions at 800 °C for 4 h. However, the ionic transport number of the composite electrolyte is as high as 0.95. This ionic transport number (t_i) was found to be almost equal to 1, which reveals the fractional contribution of ionic conductivity to the overall conductivity.

Figures 2(a) and 2(b) illustrate the ionic conductivity of the Ba-SDC electrolytes at various temperatures. The ionic conductivity of the sintered Ba-SDC sample was measured by the two-probe AC method. Figure 2(a) shows the higher proton ionic conductivity of 0.19 s/cm at 600 °C compared with conventional proton conductors in hydrogen atmosphere.

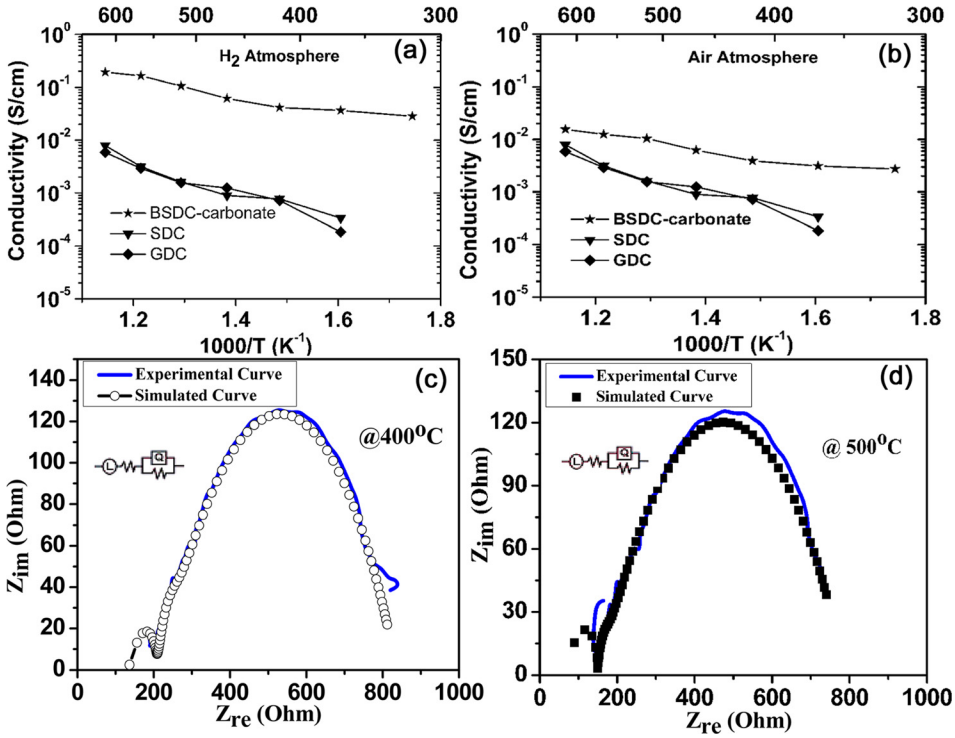

FIG. 2. Conductivity comparisons of different electrolytes SDC-carbonate, GDC-carbonate and BaSDC-carbonate in H_2 atmosphere Conductivity comparisons of different electrolytes, SDC-carbonate, GDC-carbonate and BaSDC-carbonate in air atmosphere AC impedance analysis and simulation with experimental data in H_2 atmosphere AC impedance analysis and simulation with experimental data in air atmosphere.

An oxygen ionic conductivity of 0.015 s/cm at 600 °C was recorded, which is far greater than that of conventional SDC and GDC electrolytes in ambient air atmosphere at the same temperature. In this type of fuel cell, the protons are generated on the anode side and move through the composite electrolyte towards the cathode of the cell to react with oxygen from the air, while oxygen ions move towards the anode side and pass through the composite electrolyte for oxidation. In our designed SOFC experiment, however, the proton conductivity/carrier is dominant at higher temperature and shows an isotropic effect. Therefore, it is fair to say, that the addition of BaO increased the proton carrier in this electrolyte.

EIS is usually measured by applying an AC potential to an electrochemical cell and then measuring the current through the cell. The AC impedance spectroscopy of the solid ionic conductors showed three major contributions: a high frequency arc for the bulk, an intermediate frequency for the grain boundaries, and a low frequency for the electrode behaviour. The impedance spectra of the Ba-SDC composite electrolyte in hydrogen and in air atmosphere are shown in Figures 2(c) and 2(d), respectively, at different temperatures in the range of 400–550 °C and a frequency range of 0.1 to 10 MHz under 10 mV.

The impedance spectrum of the fuel cell was measured under open-circuit conditions. In order to find the internal resistances of the fuel cell, experimental data were simulated with Z SimpWin software, and the relevant equivalent circuit was drawn for a single-phase fuel cell. The equivalent circuit contains various impedance elements representing the involved reaction steps, and the LQR parameters were found from it. L is the inductance, which indicates the effect of the stainless steel testing device and connecting cables, Q is the quality factor, and R is the resistance of the ions, electrons, and so on. The overall resistance of the cell decreases with increasing temperature, as can be observed in Figures 2(c) and 2(d).

The fuel cell performance with natural gas and hydrogen gas for the measurement of I-V (current-voltage) and I-P (current-power) densities is depicted in Figures 3(a) and 3(b), respectively. The maximum obtained power density for SOFC is 550 mW/cm^2 at 550 °C. Lower OCVs indicate that

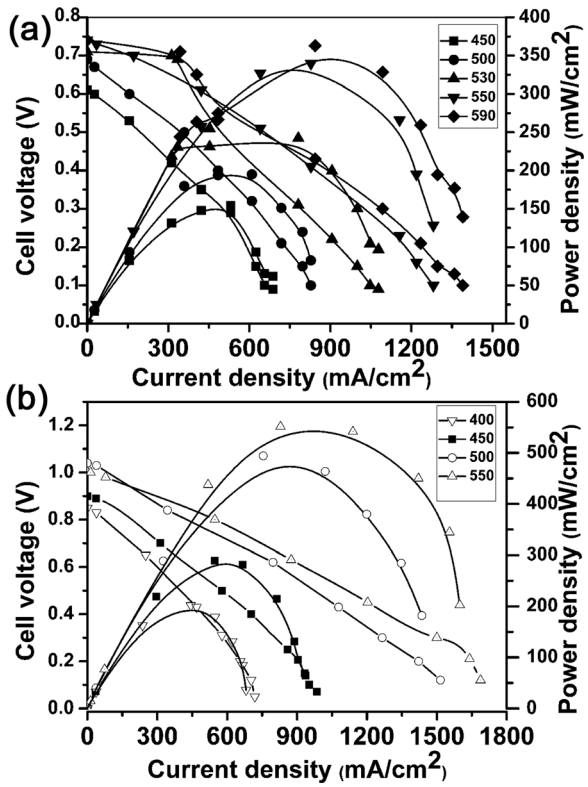

FIG. 3. (a) I-V/I-P characteristics of single cell at different temperatures with CH_4. (b) I-V/I-P characteristics of single cell at different temperatures with H_2.

the electrolyte is not gas-tight at temperatures lower than the melting point of the carbonate phase. Above the melting point, the molten carbonate phase has a good wettability to the SDC surface and fills in the pores; thus, a gas-tight electrolyte forms. This is proved by the high OCV, which is above the melting point.[21,22]

In addition, the carbonates in the composite electrolyte became molten at 500–600 °C and formed a relatively dense electrolyte layer, preventing gas crossover. However, when the operating temperature decreased to 450 °C, the carbonates became solid and formed an amount of residual pores in the composite electrolyte, leading to lower OCVs.[21–24] These results are in agreement with the observations (see Figure 3(b)).

Finally, it was found that this material can work equally well with both natural gas and hydrogen gas without compromising the performance of the fuel cell. It was observed that the above mentioned nanocomposite electrolytes were quite stable in the aggressive fuel cell environment. It was also proved that the incorporation of the Ba-SDC electrolyte significantly enhanced the performance of the fuel cell at low temperatures. Such an enhancement is mainly due to the high proton conductivity of the electrolyte; however, the proton charge carriers can decrease the interfacial resistance of the overall electrolyte/electrode of the cell. Therefore, hybrid ion conductors for LT-SOFC are considered a more attractive candidate nowadays.

We synthesized high-performance Ba-SDC dense porous nanocomposite electrolyte. The existence of nanosized crystallites in the as-prepared electrolyte was observed by XRD and SEM. The presence of nanoparticles in the perceived electrolyte allowed the thickness of the electrolyte to be decreased in the device, which helped to lower the operating temperature and improved the working conditions of the fuel cell. Our work indicates a reasonably high power density of 550 mW/cm^2 at 550 °C for the low-temperature fuel cell and proton conductivity of 0.19 s/cm at 600 °C, which is the best reported value of the hybrid ion conductivity (H^+/O^{2-}) so far.

All of the above discussed results clearly evidence the far superior properties of the nanocomposite approach for the preparation of high proton/oxygen ion conducting oxides for LTSOFCs.

A start-up research grant funded by the HEC Pakistan, COMSATS Research Grant Program (CRGP), and a research grant from the Swedish Research Council (VR, Contract No. 621-2011-4983) are gratefully acknowledged. The Netzsch Company (Germany) provided the thermal analysis. Also Imran Shakir would like to extend his sincere appreciation to the Deanship of Scientific Research at the King Saudi University for its funding of this research work through the Prolific Research Group PRG-1436-25.

[1]See http://www.era.doe.gov/oiaf/ieo/ for International Energy Outlook 2009, Energy Information Administration, Washington. DC, 2009.
[2]P. E. Hodgson, *Nuclear Power, Energy and the Environment* (Imperial College Press, 1999).
[3]X. Yunhua, D. Lele, K. Torbjorn, T. Lianpeng, L. Bao-Lin, Z. Rong, K. Bjorn, and S. Licheng, "Mononuclear ruthenium complexes that catalyze water to dioxygen oxidation," Chem. Eur. J. **17**, 9520–9528 (2011).
[4]D. Ibrahim, "Hydrogen and fuel cell technologies for sustainable future," Jordan J. Mech. Ind. Eng. **2**(1), 1–14 (2008); available at http://jjmie.hu.edu.jo/files/v2/001-v2-1.pdf.
[5]B. Viswanathan and M. A. Scibioh, *Fuel Cell Principles and Applications* (Universities Press, India, 2006); ISBN 81 7371 557 2.
[6]D. Kanno, N. Shikazono, N. Takagi, K. Matsuzaki, and N. Kasagi, "Evaluation of SOFC anode polarization simulation using three-dimensional microstructures reconstructed by FIB tomography," Electrochim. Acta **56**, 4015–4021 (2011).
[7]N. Zuo, M. Zhang, Z. Mao, Z. Gao, and F. Xie, "Fabrication and characterization of composite electrolyte for intermediate-temperature SOFC," J. Eur. Ceram. Soc. **31**(16), 3103–3107 (2011).
[8]S. Tao and J. T. Irvine, "A redox-stable efficient anode for solid-oxide fuel cells," Nat. Mater. **2**(5), 320–323 (2003).
[9]Y. Zhao, Z. Xu, C. Xia, and Y. Li, "Oxide ion and proton conduction in doped ceria-carbonate composite materials," Int. J. Hydrogen Energy **38**(3), 1553–1559 (2013).
[10]A. Elleuch, J. Yu, A. Boussetta, K. Halouani, and Y. Li, "Electrochemical oxidation of graphite in an intermediate temperature direct carbon fuel cell based on two-phase electrolyte," Int. J. Hydrogen Energy **20**, 8514–8523 (2012).
[11]J. Richter, P. Holtappels, T. Graule, T. Nakamura, and J. G. Ludwig, "Materials design for perovskite SOFC cathodes," Monatsh Chem. **140**, 985–999 (2009).
[12]B. Zhu, X. T. Yang, J. Xu, Z. G. Zhu, S. J. Ji, M. T. Sun, and J. C. Sun, "Innovative low temperature SOFCs and advanced materials," J. Power Sources **118**, 47–53 (2003).
[13]Z. Gao, J. Huang, Z. Mao, C. Wang, and Z. Liu, "Preparation and characterization of nanocrystalline Ce 0.8 Sm 0.2 O 1.9 for low temperature solid oxide fuel cells based on composite electrolyte," Int. J. Hydrogen Energy **35**(2), 731–737 (2010).
[14]J. Huang, Z. Gao, and Z. Mao, "Effects of salt composition on the electrical properties of Samaria-doped ceria/carbonate composite electrolytes for low-temperature SOFCs," Int. J. Hydrogen Energy **35**(9), 4270–4275 (2010).
[15]R. Raza, X. Wang, Y. Ma, X. Liu, and B. Zhu, "Improved ceria-carbonate composite electrolytes," Int. J. Hydrogen Energy **35**, 2684–2688 (2010).
[16]M. Jacquin, Y. Jing, A. Essoumhi, G. Taillades, D. J. Jones, and J. Rozière, "Flash combustion synthesis and characterisation of nanosized proton conducting yttria-doped barium cerate," J. New Mater. Electrochem. Syst. **10**, 243–248 (2007); available at https://hal.archives-ouvertes.fr/hal-00349615/en/.
[17]D. Medvedev, V. Maragou, E. Pikalova, A. Demin, and P. Tsiakaras, "Novel composite solid state electrolytes on the base of $BaCeO_3$ and CeO_2 for intermediate temperature electrochemical devices," J. Power Sources **221**, 217–227 (2013).
[18]E. H. Yu, U. Krewer, and K. Scott, "Principles and materials aspects of direct alkaline alcohol fuel cells," Energies **3**, 1499–1528 (2010).
[19]L. E. Smart and E. A. Moore, *Solid State Chemistry: An Introduction*, 3rd ed. (Taylor & Francis Group, 2005).
[20]R. D. Shannon, "Revised effective ionic radii and systematic studies of interatomic distances in halides and chalcogenides," Acta Crystallogr. A **32**, 751–767 (1976).
[21]J. B. Huang, Z. Q. Mao, Z. X. Liu, and C. Wang, "Development of novel low temperature SOFC with co-ion conducting SDC-carbonate composite electrolytes," Electrochem. Commun. **9**, 2601–2605 (2007).
[22]Q. Ye and T. S. Zhao, "Abrupt decline in the open-circuit voltage of direct methanol fuel cells at critical oxygen feed rate," J. Electrochem. Soc. **152**(11), A2238–A2245 (2005).
[23]J. Huang, L. Yang, R. Gao, Z. Mao, and C. Wang, "A high-performance ceramic fuel cell with samarium doped ceria-carbonate composite electrolyte at low temperatures," Electrochem. Commun. **8**(5), 785–789 (2006).
[24]C. Xia, Y. Li, Y. Tian, Q. Liu, Y. Zhao, L. Jia, and Y. Li, "A high performance composite ionic conducting electrolyte for intermediate temperature fuel cell and evidence for ternary ionic conduction," J. Power Sources **188**(1), 156–162 (2009).